Available online at www.sciencedirect.com
SCIENCE DIRECT
Lithos 90 (2006) 111–130
LITHOS
www.elsevier.com/locate/lithos

High-pressure metamorphism of the Lanzo peridotite and its oceanic cover, and some consequences for the Sesia–Lanzo zone (northwestern Italian Alps)

Laure Pelletier [a,*], Othmar Müntener [b]

[a] *Institut de Géologie, Université de Neuchâtel, Rue Emile Argand 11 CP 158, CH-2009 Neuchâtel, Switzerland*
[b] *Institut für Geologie, Universität Bern, Baltzerstrasse 1-3, CH-3012 Bern, Switzerland*

Received 12 July 2005; accepted 31 January 2006
Available online 29 March 2006

Abstract

This paper presents new data on the Alpine high-pressure evolution of the Lanzo peridotite massif and its metasedimentary cover (Western Alps). Field relations in the northwestern Lanzo massif show that the serpentinized part is covered by a metasedimentary sequence including local occurrences of metaophicarbonate, metabasalt, calcschist, metaquartzite and gneiss. Remnants of granulite-facies mafic gneiss associated with metaophicarbonate are found within the serpentinite. Major element garnet zonation profiles in metaquartzite and mafic gneiss were used to explore the contrasting origin of metasediments. Bell-shaped Mn zoning in garnet from metaquartzite indicates a one-stage Alpine metamorphic evolution, while inverse zoning in garnet of the mafic gneiss shows that the protolith equilibrated under high-grade metamorphic conditions in pre-Alpine times, similar to kinzigites within the neighbouring Sesia zone. Phase equilibria in metaquartzite and mafic gneiss point to 500±50 °C at pressures of 0.9 to 1.3 GPa for the Alpine metamorphic equilibration that contrasts with the 550–620 °C and pressures in excess of 2.0 GPa obtained for kyanite+talc+chloritoid and talc+chloritoid+garnet domains in a metagabbro dike from the internal part of the Lanzo massif. These different *P–T* trajectories can be explained by a much stronger retrograde overprint at the basement–cover contact than in the internal part of the Lanzo massif.

Keywords: Eclogite facies metamorphism; Kyanite–talc metagabbro; Granulite; Lanzo peridotite; Sesia–Lanzo zone; Western Alps

1. Introduction

Ever since the recognition that some of the ophiolites preserved in the Alps are fossil records of a Mesozoic ocean–continent transition, the high-pressure rocks of the Western Alps have been the subject of some debate. The close association of granulites and ancient oceanic lithosphere was interpreted as an analogue of present-day ocean–continent transitions (Froitzheim et al., 1996) that were subjected to high-pressure metamorphism in the late Cretaceous–Early Tertiary (Rubatto et al., 1999). On the contrary, the ophiolites preserved in the Western Alps are generally regarded as high-pressure analogues of modern slow-spreading ridges (e.g. Lagabrielle et al., 1984; Lagabrielle and Cannat, 1990).

* Corresponding author. Tel.: +41 32 7182680; fax: +41 32 7182601.
E-mail address: laure.pelletier@unine.ch (L. Pelletier).

0024-4937/$ - see front matter © 2006 Elsevier B.V. All rights reserved.
doi:10.1016/j.lithos.2006.01.006

Of particular interest for the paleogeography and for the early high-pressure metamorphic evolution of the Piemontese–Ligurian ocean is the mutual relationship of oceanic and continental units and their Mesozoic cover. It is well established that the internal parts of Piemontese ophiolites and the continental Sesia zone were subducted to eclogite facies conditions, with the highest pressures and temperatures preserved in the most internal parts, e.g. in the eclogitic micaschists (EM) of the Sesia zone (550–620 °C, 1.3–2.0 GPa: e.g. Compagnoni, 1977; Pognante, 1989; Lardeaux and Spalla, 1991) and in metagabbros of the Lanzo peridotite (450–500 °C, 1.5–1.8 GPa, Kienast and Pognante, 1988). It was proposed that the Sesia zone and the Lanzo peridotite experienced a common Alpine high-pressure deformation history (Spalla et al., 1983). If so, one might assume that (i) primary (pre-high pressure) field relationships might be preserved, (ii) similar peak metamorphic conditions should be recorded in both units, and (iii) that the apparent 'gradient' in peak metamorphic pressures and temperatures established for the Sesia zone (decreasing peak conditions from the internal to the external part of the Sesia zone, e.g. Pognante, 1989) should also be recorded by the Lanzo peridotite.

The key to understanding if and how the peridotite of the Lanzo massif, the continental crust of the Sesia zone and metasediments are connected and record the same pressure–temperature evolution during the Alpine subduction cycle, must be constrained by field and petrological data in the northwestern part of the Lanzo massif, where the 2 units merge. Available data suggest that the Lanzo massif was emplaced at shallow levels during the Mesozoic (e.g. Pognante et al., 1982, 1985; Bodinier et al., 1986; Lagabrielle et al., 1989) and later, it was subducted and partially recrystallized at eclogite facies conditions (Kienast and Pognante, 1988). Similarly, monometamorphic metasedimentary successions covering orthogneisses in the more external parts of the Sesia zone (the gneiss minuti complex (GM), Spalla et al., 1983; Pognante, 1989) indicate shallow level exposure of continental crust in mid to upper Jurassic time.

The purpose of this study is to establish the lithostratigraphy of the metasedimentary cover and its relationships to the Lanzo ultramafic rocks and to the continental rocks of the Sesia zone. We investigate textural and chemical variations in metagabbro, metaquartzite and gneiss to determine peak metamorphic assemblages. In addition, we estimate the P–T conditions for the equilibration of kyanite with talc +chloritoid in metagabbro through thermodynamic calculations and discuss potential reasons for the P–T discrepancy of basement and oceanic cover in the Lanzo peridotite. Finally, we discuss the significance of lower crust remnants within the Lanzo peridotite and evaluate the possibility of a Mesozoic 'ocean–continent transition' for the Sesia–Lanzo connection.

2. Geological setting of the Lanzo peridotite

The Lanzo ultramafic body (~150 km^2) is located in the Western Alps bounded by Po plain sediments to the east and south, high-pressure meta-ophiolites and schistes lustrés to the West, and continental units of the Sesia–Lanzo zone in the North (Fig. 1, Nicolas, 1974; Spalla et al., 1983; Pognante, 1989). The massif predominantly consists of plagioclase lherzolite, with minor spinel lherzolite, pyroxenite and dunite, surrounded and partially cut by serpentinite (e.g. Boudier, 1978). Its origin has been widely debated in the late 1970s and early 1980s, the position of the lherzolite body being the 'triple junction' between the Penninic ophiolites, Austroalpine units and the Ivrea–Verbano zone. Early interpretations suggested a direct relationship with Ivrea mantle rocks, apparently corroborated by the gravimetric anomaly of the Ivrea body, which is also measurable in the Lanzo area and postulated an emplacement during Alpine collision (Nicolas, 1974). Geochemical and petrological data obtained by Lombardo and Pognante (1982), Pognante et al. (1985), Bodinier et al. (1986), Bodinier (1988) and Piccardo et al. (2004) showed that MORB-type basaltic dikes intrude the ultramafic body suggesting an oceanic origin for the Lanzo mantle, in agreement with the interpretation of a close relationship between Alpine plagioclase lherzolites and the opening of the Piemontese-Ligurian basin (Beccaluva et al., 1984; Nicolas, 1986). Metarodingite dikes within the serpentinized part of the Lanzo massif further corroborated the hypothesis of an oceanic genesis (Pognante et al., 1985). The Alpine high-pressure metamorphism of the Lanzo peridotite is heterogeneous. Large volumes show incipient high-pressure eclogite facies overprint in metagabbros (Kienast and Pognante, 1988) and in the oceanic cover (Lagabrielle et al., 1989). Only the borders of the Lanzo massif are affected by pervasive metamorphic equilibration (Kienast and Pognante, 1988).

The Sesia zone is a composite continental basement consisting of 3 different tectonic subunits (Fig. 1, Dal Piaz, 1999): an upper continental crust and their Mesozoic sedimentary cover (gneiss minuti complex, GM), polymetamorphic gneisses and schists derived from pre-Alpine lower crust (seconda zona diorito-

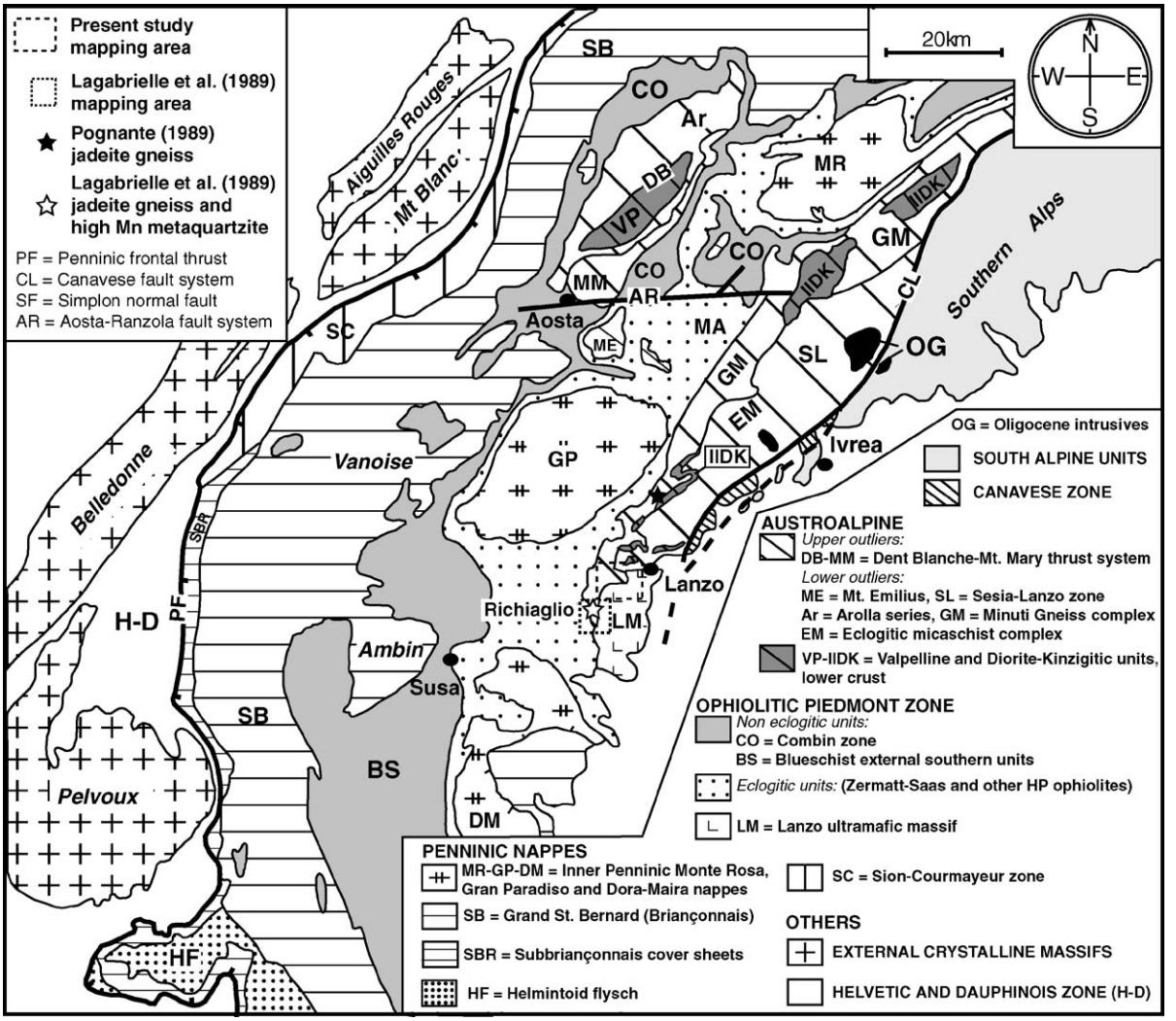

Fig. 1. General tectonic overview of the Western Alps (modified after Dal Piaz, 1999) and location of the Lanzo massif. Southern IIDK units localized after Pognante (1989). Stars indicate jadeite-bearing gneisses in the gneiss minuti complex (GM) of the Sesia zone (Pognante, 1989) and jadeite-bearing gneisses and manganiferous garnet metaquartzites in the oceanic cover of the Lanzo massif (Lagabrielle et al., 1989).

kinzigitica, IIDK) and eclogitic micaschists (EM) consisting of Paleozoic intrusives, mafic rocks and rare high-grade metasediments. As for the Lanzo peridotite, the high-pressure recrystallization is rarely pervasive, and ubiquitous relics of the pre-Alpine history are preserved. The highest pressures and temperatures related to Alpine metamorphism are recorded in the most internal parts, e.g. in the eclogitic micaschists (550–620 °C, 1.3–2.0 GPa: Compagnoni, 1977; Williams and Compagnoni, 1983; Pognante, 1989; Lardeaux and Spalla, 1991). According to Pognante (1989), slightly lower conditions were found in the gneiss minuti complex (GM) of the Southern Sesia–Lanzo zone (400–450 °C and ≥1.1–1.2 GPa). Some authors argue that pressures never have been high enough in the GM to produce albite breakdown (Wheeler and Butler, 1993; Inger and Ramsbotham, 1997; Desmons et al., 1999), but Pognante (1989) mentioned the presence of a jadeite-quartz bearing orthogneiss (Southern Sesia–Lanzo zone, Fig. 1) in this unit. After the high-pressure peak, the GM and EM followed retrogression under blueschist and greenschist facies, illustrating near isothermal exhumation or cooling during uplift.

3. Petrography, mineral assemblages and microstructures

Detailed mapping at a scale of 1:10,000 revealed a series of metamorphosed oceanic rocks covering the

ultramafic rocks of the northern and central areas between Pugnetto and Viù (Fig. 2). This succession includes from bottom to top: metaophicarbonate, metabasalt, phengite–quartz calcschist and marble, and chlorite–phengite gneiss. Phengite–garnet–chlorite metaquartzite was found in the northern area near Pugnetto and is associated with calcschist (Fig. 2). A similar lithostratigraphy (metabasalt, calcschist, phyllitic garnet-bearing metaquartzite, phyllitic marble with eclogite facies basaltic pebbles, fine-grained leucocratic

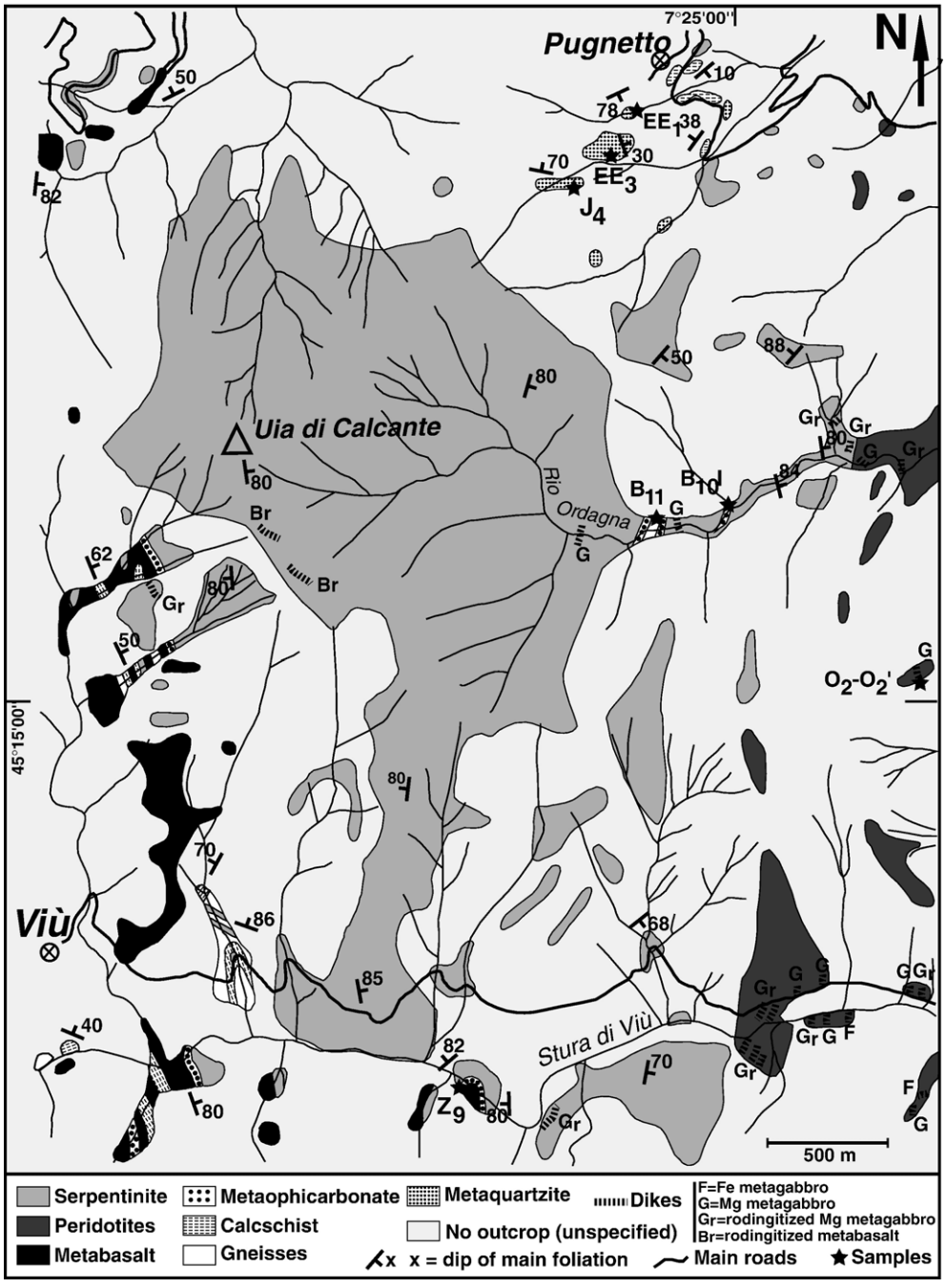

Fig. 2. Simplified geological map of the Northwestern part of the Lanzo massif, illustrating serpentinite-sedimentary cover contacts and the occurrence along the contact of a succession with metaophicarbonate, metabasalt, chlorite–phengite gneiss, phengite–quartz calcschist. Stars: samples used for microprobe and SEM investigations. O_2 and O_2' are two different thin sections of the same sample.

gneiss) was described by Lagabrielle et al. (1989), near the village of Richiaglio (Fig. 1). Regional deformation generated four deformation phases, including isoclinal folding (Spalla et al., 1983). In some regions, the oceanic succession is incomplete because of either Alpine thrusting or by original lateral variations.

3.1. Ultramafic rocks

Mantle rocks are dominated by plagioclase lherzolite with minor dunite, spinel lherzolite and pyroxenite (Boudier, 1978; Pognante et al., 1985; Bodinier, 1988; Müntener and Piccardo, 2003). The peridotite core is surrounded by serpentinized peridotite and strongly foliated serpentinite, mainly composed of antigorite and diopside, and minor olivine, chlorite, magnetite and titanian-clinohumite. In places the top of the mantle rocks is covered by ophicarbonate breccias (Fig. 3).

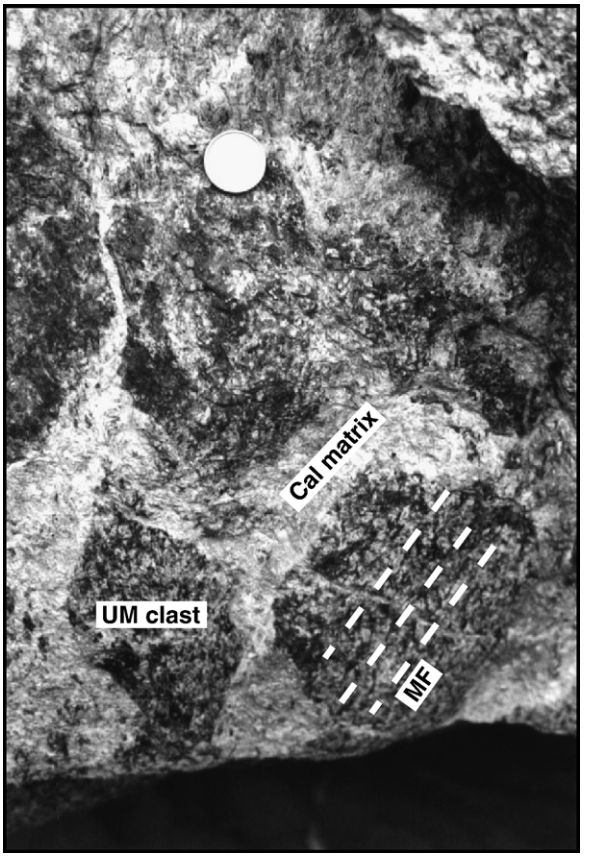

Fig. 3. Field aspect of metaophicarbonate, illustrating ultramafic (UM) clasts in a calcitic (Cal) matrix. The tectonite foliation (MF) of the former peridotite is still recognizable.

3.2. Metagabbro dikes

Numerous gabbroic dikes intruded the massif, ranging from troctolite, olivine gabbro to oxide gabbro (Nicolas, 1966; Pognante et al., 1985; Bodinier, 1988). Basaltic intrusions are frequent (Nicolas, 1966; Pognante et al., 1985; Bodinier et al., 1986; Bodinier, 1988) and some rare plagiogranite were described (Pognante et al., 1984). Primitive Mg-rich gabbro dikes have a chemical composition of cumulates (Bodinier et al., 1986). Some gabbros were partially transformed into eclogite facies metagabbros during Alpine metamorphism. Depending on the whole rock chemistry (Mg gabbro or oxide gabbro), different high-pressure mineral parageneses developed (Kienast and Pognante, 1988). Our samples are different from previously studied ones as they show cumulus and intercumulus domains inherited from igneous crystallization. These microchemical domains developed different metamorphic parageneses within the same sample. In the olivine domain, talc+kyanite+chloritoid formed, with chloritoid often outlining the olivine-plagioclase boundary (Fig. 4A,B). In domains slightly richer in Fe, talc+chloritoid+garnet+rutile formed (Fig. 4C). The plagioclase domain is essentially formed by zoisite, no Na-pyroxene or quartz has been observed. Igneous clinopyroxene is partially pseudomorphosed by diopside, associated with talc, rutile and omphacite. Omphacite is present as an inclusion in relic diopside (Pelletier, 2003; see also Kienast and Pognante, 1988). Na-amphibole has not been found. Between the former cumulus phases, apatite and ilmenite (now transformed to rutile +almandine component in garnet) were present. Replacement of ilmenite by rutile is indicated by the hexagonal geometry of the rutile needles (Fig. 4B). The general absence of jadeite in the plagioclase domain and the rare occurrence of omphacite indicate that the bulk composition of the igneous protolith was Na-poor.

Some gabbro dikes are partially transformed into metarodingites (Fig. 2). They can be distinguished from metarodingites of basaltic origin by the preservation of the coarse grain size. Rodingitization most probably occurred during exposure of the ultramafic rocks on the ocean floor by circulation of fluids connected to serpentinization of mantle rocks, which increased the Ca and decreased the Na contents of the bulk rock (e.g. Evans et al., 1979). The primary rodingitic mineralogy was modified during high-pressure metamorphism leading to a new mineral assemblage with Ca–Fe-rich garnet, diopside, chlorite, epidote, titanite and tremolite.

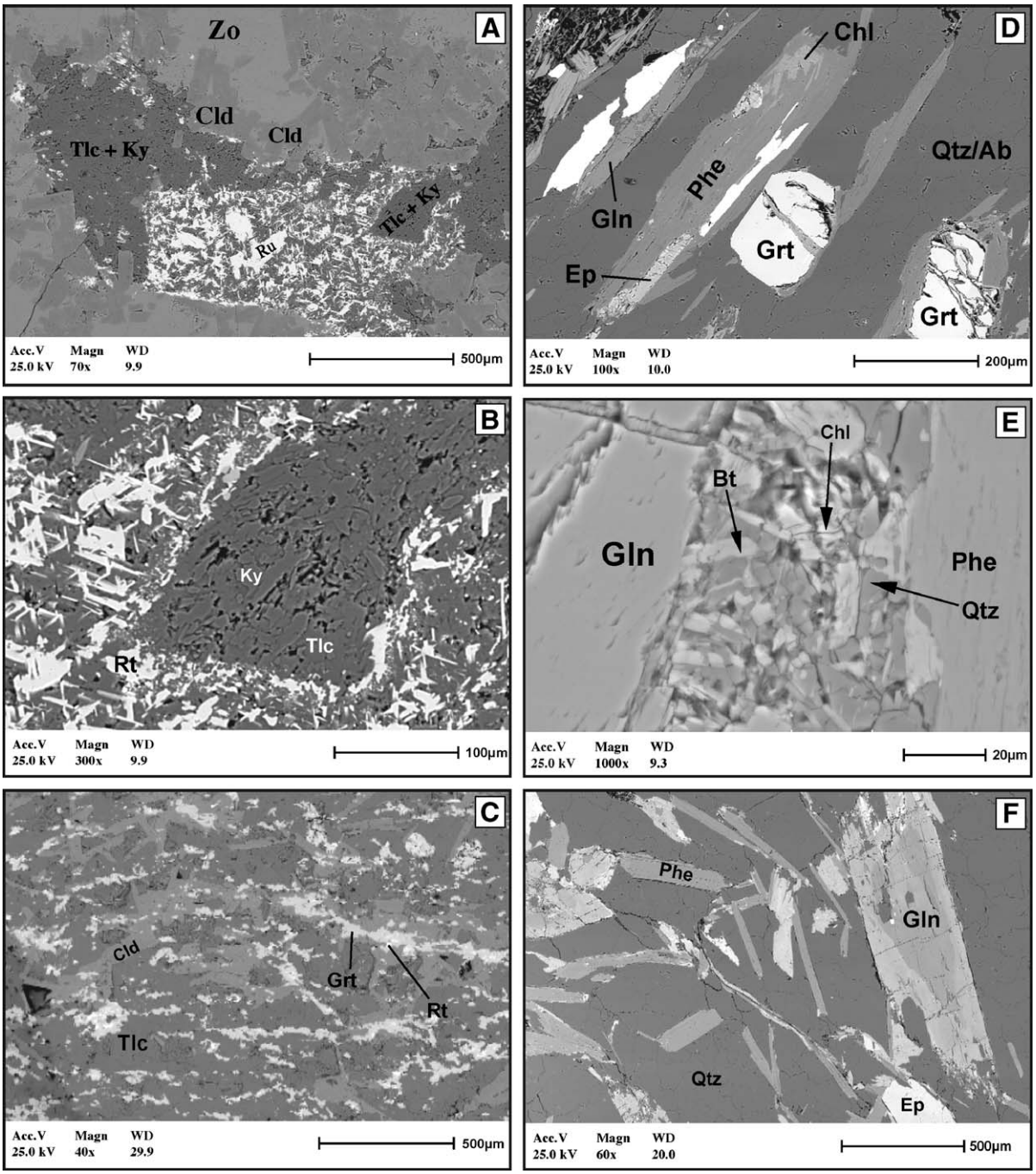

Fig. 4. BSE images of metagabbro and metaquartzites used for thermobarometric estimates. (A) Tlc+Ky+Cld rim around Rt+Tlc core in a Mg-rich domain of kyanite–talc metagabbro O_2'. (B) Detail of (A) on the Tlc+Ky area indicating microstructural equilibration between Ky and Tlc. (C) Details on the Tlc+Grt+Cld assemblage of kyanite–talc metagabbro O_2'. (D) Illustration of the high-pressure paragenesis Phe+Grt+ Gln +Qtz in metaquartzite J_4. (E) Retrograde assemblage Bt+Chl+Qtz in a symplectite of metaquartzite EE_3 indicating a retrograde reaction of Phe +Tlc→Bt+Chl+Qtz. (F) Glaucophane zoning in metaquartzite EE_3. The brighter rim is Ca-richer (see Table 2). (Ab=albite, Bt=biotite, Chl=chlorite, Cld=chloritoid, Ep=epidote, Gln=glaucophane, Grt=garnet, Ky=kyanite, Phe=phengite, Qtz=quartz, Rt=rutile, Tlc=talc, Zo=zoisite.)

Two types of vesuvianite are present, the first one is euhedral and formed in veins cutting the metarodingite, while the second generation of vesuvianite partially replaces the high-pressure assemblage.

3.3. Metaophicarbonate

Metaophicarbonate was found in five localities along the mantle–cover contact and in one outcrop within the ultramafic rocks close to a phengite–gneiss along the Ordagna river (Fig. 2). They are found on top of the serpentinized mantle rocks, contain rounded clasts of ultramafic components varying in size from millimeter to decimeter scale, embedded in a carbonate matrix (Fig. 3). Ultramafic minerals are partially replaced by carbonates, but a relic mantle structure is still recognizable (Fig. 3). The stable paragenesis is calcite + tremolite + antigorite. Dolomite is present as a relic inside calcite grains and diopside is often surrounded by a tremolite corona. These rocks indicate that the Lanzo mantle rocks were, at least partially, exposed on the Tethyan ocean floor, as previously suggested by Lagabrielle et al. (1989).

3.4. Metabasalt

These rocks are characterized by a greenish color in the field and directly cover either underlying serpentinite or metaophicarbonate. The matrix is mainly composed of chlorite but the main characteristic feature is albite porphyroblasts with a maximum size of 1 mm. The mineral assemblage in these rocks (mainly chlorite, titanite, albite, actinolite and epidote) indicates greenschist facies conditions. However, relics of almandine, rutile, phengite, glaucophane and zoisite, which are included in greenschist facies minerals, indicate a precursor blueschist or eclogite facies metamorphism.

3.5. Phengite–garnet–chlorite metaquartzite

Metaquartzite was observed in the northern area near Pugnetto, and further south near Richiaglio (Lagabrielle et al., 1989) and also on top of the Civrari ophiolite (Défago, 2004). Metaquartzite contains at least 70% quartz, with variable amounts of garnet, epidote, glaucophane, phengite, chlorite, albite and actinolite. Accessory minerals are apatite, allanite, tourmaline and rare carbonates. Chlorite may be present in the matrix, but also as corona around garnet.

A high-pressure paragenesis is documented by the assemblage phengite + garnet + glaucophane + quartz ± allanite. A lower pressure assemblage includes chlorite + Mg-riebeckite + quartz + albite + epidote + biotite. Backscattered electron (BSE) images show the presence of a chlorite + biotite + quartz symplectite inside or at the rim of glaucophane (Fig. 4E). Symplectitic intergrowths were probably formed from phengite + talc during retrogression (Massonne and Schreyer, 1989).

3.6. Chlorite–phengite gneiss

Different types of gneiss were mapped in different localities along the mantle-cover contact (leucocratic paragneiss) and inside the serpentinized part of the Lanzo massif (phengite-bearing mafic gneiss, sample B_{11}, Fig. 2). In the first type of gneiss (paragneiss), high-pressure relics are phengite, zoisite, rare garnet and glaucophane. Glaucophane (~5 μm) is present as a relic in actinolite and can only be found by scanning electron microscopy. Retrograde recrystallization formed a greenschist facies mineral assemblage albite + chlorite + titanite + epidote + actinolite. Accessory minerals are biotite, rare carbonate, allanite and pyrite. A characteristic feature is the presence of chlorite + epidote + phengite pseudomorphs after glaucophane. Jadeite has never been observed in the studied area, but the assemblage jadeite + quartz was described by Lagabrielle et al. (1989) indicating that the gneiss recrystallized at eclogite facies conditions.

A phengite-bearing mafic gneiss with irregular quartz veins was found within the serpentinite along the Ordagna river (sample B_{11}, for location see Fig. 2) and is separated from the serpentinite by an intensely foliated metaophicarbonate zone about 10 m wide. The quartz-rich layers form discontinuous and thin slices between more mafic parts. The gneiss is characterized by a greenschist facies mineral assemblage, consisting of chlorite, actinolite, epidote, titanite and albite porphyroblasts. High-pressure relics are phengite, glaucophane (only present in actinolite core), garnet rims around pre-Alpine garnet-porphyroclasts, quartz, rutile and zoisite. Accessory zircon crystals are abundant in this rock. The intercalation of phengite-bearing mafic gneiss, metabasic rocks and quartz-rich veins is similar to the 'polymetamorphic paraschists' of Pognante (1989). The association is equivalent to rocks known in the IIDK in the Sesia zone.

3.7. Calcschist

Calcschist is characterized by alternating layers of impure marble and micaschist varying at a cm to dm

scale. Impure marble is dominated by calcite, with minor amounts of garnet, rutile, phengite, epidote, chlorite and titanite. Micaschist is dominated by phengite, chlorite and quartz, with minor albite, chlorite, tourmaline and apatite. These rocks are found all along the mantle-cover contact (Fig. 2).

4. Mineral chemistry

Mineral compositions were determined using a Cameca SX-50 electron microprobe located at the Institute of Geological Sciences at the University of Bern (Switzerland), equipped with four wavelength-dispersive spectrometers. Operating conditions comprised an acceleration voltage of 15 kV and a 20 nA beam current. The spot size was about 3 μm for all minerals except phengite, chlorite and biotite, where a defocused beam has been used (~10 μm). Element peak and background counting time was 20 s, except for Al (30 s), Mg (30 s) and Na (10 s). Natural and synthetic oxides were used as standards. Backscattered electron (BSE) images were obtained at the Centre Suisse d'Electronique et de Microtechnique (CSEM) in Neuchâtel (Switzerland), with an Environmental Scanning Electron Microscope, Philips XL-30, operated at 25 kV.

Table 1
Representative electron microprobe analyses of high-pressure minerals in kyanite–talc metagabbro

Sample	Cld	Cld	Grt	Grt	Grt	Tlc	Tlc	Ky	Omp	Omp	Omp	Zo
	O_2'	O_2'	O_2'	O_2'	O_2'	O_2'	O_2'	O_2'	O_2'	O_2'	O_2'	O_2'
	Mg-rich area	Fe-rich area			Mg-rich area	Fe-rich area						
wt.%												
SiO_2	25.7	25.0	38.1	38.4	38.9	64.0	62.7	37.5	57.3	57.0	56.7	39.3
TiO_2	<0.01	<0.01	0.10	0.12	0.32	0.02	<0.01	0.06	0.24	0.38	0.28	0.03
Al_2O_3	43.2	43.1	21.5	21.1	21.5	0.49	0.43	61.7	12.3	13.5	11.3	32.9
Cr_2O_3	<0.01	<0.01	<0.01	<0.01	<0.01	0.02	<0.01	0.01	0.01	0.04	0.03	<0.01
Fe_2O_3			1.06	1.23								0.93
FeO	11.8	14.4	23.1	21.9	24.8	2.02	2.78	0.07	1.28	1.09	1.21	
MnO	0.09	0.09	0.89	0.41	0.44	0.02	0.03	0.02	<0.01	0.07	<0.01	<0.01
CaO	<0.01	0.03	12.2	12.9	10.4	0.01	0.02	0.02	12.6	11.0	13.3	24.2
Na_2O	0.01	0.01	0.01	0.06	0.06	0.03	0.05	0.04	7.46	8.65	7.33	0.04
K_2O	<0.01	<0.01	0.01	0.01	0.03	0.01	<0.01	0.02	<0.01	0.02	0.03	0.03
H_2O	7.67	7.61				4.67	4.70					1.97
Sum	99.1	99.5	100.3	99.9	100.6	100.7	100.2	99.8	100.0	99.6	99.5	99.5
Cations normalized to	14 oxy	14 oxy	12 oxy 8 cations	12 oxy 8 cations	12 oxy 8 cations	12 oxy	12 oxy	5 oxy	6 oxy 4 cations	6 oxy 4 cations	6 oxy 4 cations	12 oxy 1 OH
Si	2.005	1.972	2.975	2.993	3.012	4.009	3.996	1.015	2.003	1.997	1.999	2.998
Ti	0.005	0.002	0.006	0.007	0.018	0.001		0.001	0.006	0.010	0.007	0.002
Al	3.973	4.002	1.979	1.938	1.966	0.036	0.032	1.967	0.507	0.557	0.470	2.947
Cr						0.001	0.000	0.000		0.001	0.001	
Fe^3			0.062	0.072								0.053
Fe^2	0.771	0.951	1.507	1.430	1.605	0.106	0.148	0.002	0.037	0.032	0.036	
Mn	0.006	0.006	0.058	0.027	0.029	0.001	0.002	0.001		0.002		
Mg	1.243	1.089	0.390	0.441	0.497	2.815	2.806	0.011	0.459	0.408	0.491	0.015
Ca		0.003	1.020	1.082	0.860	0.001	0.001	0.001	0.472	0.413	0.502	1.981
Na	0.002	0.002	0.002	0.009	0.010	0.004	0.007	0.002	0.505	0.587	0.501	0.007
K			0.002	0.001	0.003	0.001		0.001		0.001	0.001	0.003
H	4.000	4.000				2.000	2.000					1.000
# cations	8.004	8.026	8.000	8.000	7.999	6.974	6.992	3.001	3.990	4.008	4.009	8.005
Mg# (Fe^{2+})	0.617	0.534	0.205	0.236	0.237	0.964	0.950	0.879	0.925	0.927	0.932	
Mg# (Fe_{tot})	0.617	0.534	0.199	0.227	0.237	0.964	0.950	0.879	0.925	0.927	0.932	
Fe^{3+}/Fe_{tot}	0.000	0.000	0.040	0.048	0.000	0.000	0.000	0.000	0.000	0.000	0.000	0.000
Al(IV)			0.025	0.007	0.000				0.000	0.003	0.001	0.002
Al(VI)			1.954	1.931	1.966				0.507	0.554	0.469	2.945

Fe^{3+} and water content were calculated stoichiometrically (without measurement of F, Cl and other anions for water content estimation). (Cld=chloritoid, Grt=garnet, Tlc=talc, Ky=kyanite, Omp=omphacite and Zo=zoisite; oxy=oxygens.

4.1. Kyanite–talc metagabbro dike (samples O_2 and O_2')

Representative mineral compositions of the kyanite–talc metagabbro dike are listed in Table 1, and some of the phase relations are shown in Fig. 5.

Chloritoid is Mg-rich with Mg# (Mg/[Mg+Fe_{tot}]) between ~0.53 and ~0.63, with higher ratios in Mg-rich domains in the presence of talc and kyanite and lower values in domains equilibrated with garnet+talc±rutile (Fig. 5). In both assemblages chloritoid is euhedral, and forms preferentially at the contact between talc+kyanite patches (former olivine site) and zoisite (former plagioclase site). Chloritoid was probably formed by the H_2O conserving solid–solid reaction:

$$\text{chlorite} + \text{kyanite} = \text{chloritoid} + \text{talc}. \quad (1)$$

Reaction (1) was experimentally investigated by Chopin and Schreyer (1983) and Koch-Müller and Wirth (2001). In our samples, however, we were unable to find chlorite. Mg-chloritoid compositions are similar to those determined by Kienast and Pognante (1988), however, the latter authors found chlorite instead of kyanite as a coexisting phase.

Talc is nearly stoichiometric with Mg# varying between 0.95 (coexisting with chloritoid and garnet) and 0.97 (coexisting with kyanite). It contains moderate amounts of Al_2O_3 (Table 1).

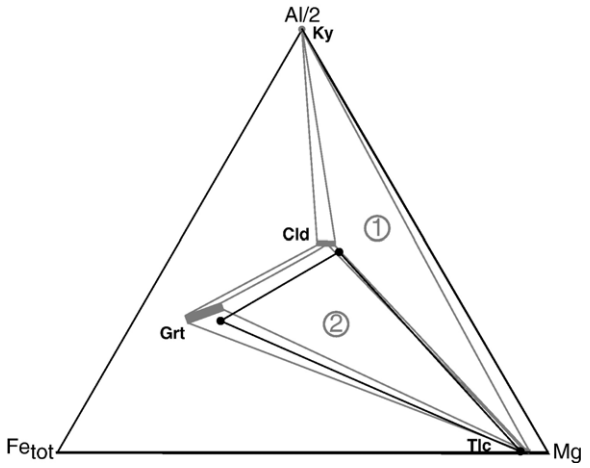

Fig. 5. AFM (Al/2, Fe_{tot}, Mg) diagram illustrating stable high-pressure mineral assemblages in the kyanite–talc metagabbro O_2'. Grey: parageneses observed in present study. (1) Ky+Cld+Tlc and (2) Grt+Cld+ Tlc. Black: paragenesis Grt+Cld+Tlc of Kienast and Pognante (1988). (Cld=chloritoid, Grt=garnet, Ky=kyanite and Tlc=talc.)

Kyanite has, to the best of our knowledge, been found for the first time in the Lanzo massif. Its composition is uniform and contains small amounts of Mg and Fe (Table 1). Kyanite is quite small (<50 μm, Fig. 4B), anhedral and intimately intergrown with talc.

Garnet composition is rather uniform and rich in almandine (~$Gross_{34}Alm_{52}Pyr_{13}$). Overall, garnet has a composition similar to those presented by Kienast and Pognante (1988) (see also Fig. 5). They are never found to be in equilibrium with omphacite. No systematic variations between core and rim could be detected and this absence of a more prominent growth zonation might indicate that garnet equilibrated with chloritoid in a narrow pressure–temperature interval.

Zoisite is nearly stoichiometric and contains less than 1% Fe_2O_3 independent on the microstructural site.

Omphacite occurs as inclusion in diopside and is Mg-rich (Mg#>0.92), with jadeite fractions varying between 0.50 and 0.55 (Table 1).

4.2. Metasedimentary rocks (samples B_{11}, EE_3 and J_4)

Most of the minerals in the metasedimentary rocks show compositional zoning, most notably garnet (Fig. 6) and amphibole (Fig. 7). Representative mineral compositions of metaquartzites are reported in Table 2, while analyses of chlorite–phengite gneiss B_{11} are listed in Table 3.

Garnets plot on the almandine (+pyrope)–spessartine join and have low grossular contents (Fig. 8, Tables 2 and 3). Euhedral garnet from the metaquartzite shows characteristic 'prograde' zoning patterns with spessartine-rich compositions in the core. Garnet with up to ~35 mol% spessartine component in the core was determined (Fig. 6A). In similar rocks near Richiaglio garnet with up to 90 mol% spessartine has been described (Fig. 8, Lagabrielle et al., 1989). Garnet is zoned with a decrease of Mn and Ca contents rimward and an increase of the Mg# (Fig. 6A). The Mn-rich nature of the garnets probably illustrates a (local) hydrothermal enrichment of Mn in metaradiolarites, similar to other metamorphosed radiolarite occurrences in other parts of the Alps (e.g. Peters et al., 1973; Reinecke, 1998). On the contrary, garnet from the chlorite–phengite gneiss shows little zoning and has small rims with decreasing Mg# and increasing grossular and spessartine contents. Most notably, the cores show a large plateau of nearly constant composition (Fig. 6B), high pyrope and very low grossular contents (Table 3), similar to some garnets from the

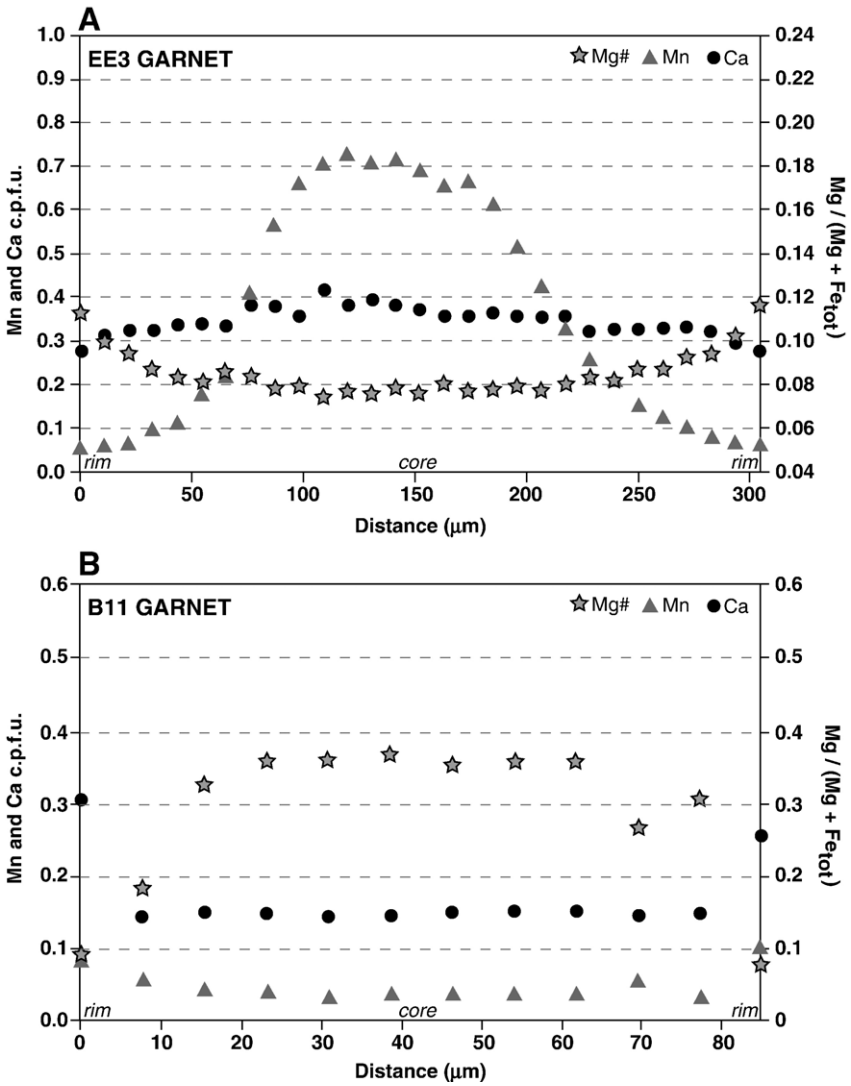

Fig. 6. Mn and Ca contents per formula unit and Mg# (Mg/[Mg + Fe_{tot}]) compositional profiles in a high-pressure garnet of metaquartzite EE_3 (A) and chlorite–phengite gneiss B_{11} (B). Note the bell-shaped distribution of Mn in the metaquartzite indicating one-stage crystallization during garnet growth. On the contrary, garnets from the gneiss show high Mg# in the core and low Ca and Mn contents, suggesting previous high-temperature equilibration (for sample location, see Fig. 2).

high-temperature granulite-facies basement rocks in the Sesia zone (IIDK or polymetamorphic paraschists: Pognante, 1989). The Ca-increase towards the rim (as shown in Fig. 8) is common in most eclogites from the Sesia zone (e.g. Pognante, 1989) and indicates an Alpine high-pressure overprint on granulite facies garnet relics.

Phengite has a variable, but high celadonite component (Tables 2 and 3). In metaquartzite lepidoblastic phengite (Fig. 4F) shows Si contents between ~3.52 and 3.56 (c.p.f.u.), whereas in symplectite, values of ~3.57 to 3.61 were measured. Phengite from the gneiss is rather homogeneous, with no significant compositional variations from the core to the rim (Si: 3.45 to 3.52). The (Mg+Fe) content of analyzed phengite is always higher than required by the pure celadonite substitution, indicating some biotite solid solution. In all samples phengite is the most magnesian phase ($Mg\#^{phe} > Mg\#^{gln} \gg Mg\#^{grt}$), with Mg# of ~0.64 in metaquartzite, and ~0.70 in gneiss, respectively. Na contents are below 0.15 wt.%.

Na-amphibole of metaquartzite is a nearly Ca-free glaucophane in the core overgrown by a Ca-bearing Mg-

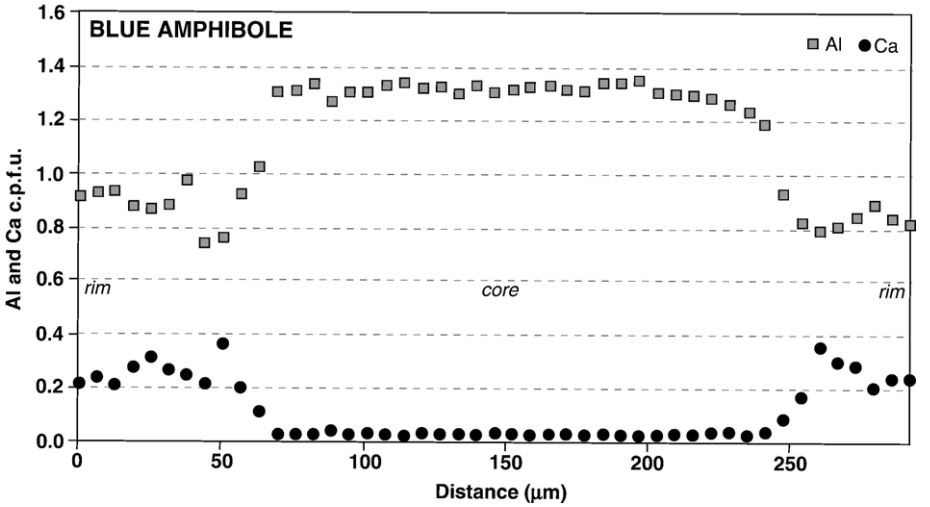

Fig. 7. The variation of Al and Ca contents (in cations per formula unit) in profiles across blue amphibole of metaquartzite J_4 (for sample location, see Fig. 2). Ca and Al are homogeneous throughout the core illustrating equilibrium crystallization during the peak metamorphic conditions, followed by a retrograde reequilibration under blueschist to greenschist facies conditions leading to a rimward decrease in Al and an increase in Ca, respectively.

riebeckite at the rim (nomenclature according to Leake et al., 2004). The Mg# decreases from ~0.60 in the core to ~0.53 along the rims. Na_2O decreases rimward with a value of ~7.11 wt.% in the core and ~6.50 wt.% at the rim (Fig. 7).

Chlorite partially replacing garnet is common in both metaquartzite and gneiss and is fairly rich in Fe (Tables 2 and 3). In symplectite bordering phengite and glaucophane (Fig. 4E), chlorite intergrown with biotite and quartz shows significantly higher Mg# values covering a range between 0.60 and 0.64.

Biotite rimming phengite and forming symplectitic intergrowths with chlorite and quartz was only found in metaquartzite and is low in Ti and Na (Table 2). Mg# values (~0.58) are somewhat lower than that of coexisting chlorite (Mg# ~0.60 to 0.64).

5. Thermobarometry

5.1. Thermobarometry of kyanite–talc metagabbro dike

At pressures above the amphibole-out reaction, K- and Ti-poor basaltic and gabbroic rocks can be modeled in the Na_2O-CaO-FeO-MgO-Al_2O_3-SiO_2-H_2O (NCFMASH) system. In the studied samples, Ti appears only in rutile and thus the abundance of rutile is controlled by the bulk composition. The same is true for Na, which is present only in the jadeite component of (rare) omphacite; no Na-amphibole has been found. The total amount of jadeite is thus fixed by the bulk composition and remains unbuffered in omphacite. Inspection of SEM images further shows that the gabbroic rocks are controlled by local rather than by bulk rock equilibria (see also Kienast and Pognante, 1988).

First, we considered the Ca-poor microchemical domains (former olivine sites in fresh, unaltered Mg gabbros), which may be modeled in a FeO-MgO-Al_2O_3-SiO_2-H_2O (FMASH) system: bulk compositions of the two different domains are obtained by modal analyses of SEM images and the appropriate mineral compositions listed in Table 2. They were recalculated on an atom basis and are given on top of Fig. 9. Phase diagrams were calculated employing the database of Berman (1988), updated with revised thermodynamic properties of Fe-Chloritoid (Vidal et al., 1999) and Mg-Chloritoid (Vidal et al., 2001). An ideal solution model was adopted for the Fe–Mg exchange in chloritoid and talc. The model of Hunziker (2003) was used for chlorite solid solutions, and Berman's (1990) model was chosen for garnet solid solutions. Recently published thermodynamic data for Fe-chlorite by Parra et al. (2005) and Vidal et al. (2005) are similar (<2.5% relative difference for S_0, H_0 and V_0 for Fe-amesite, respectively) to those derived by Hunziker (2003). Using these data for chlorite does not significantly change our results. All calculations have been made at H_2O saturation, a reasonable assumption since the gabbroic dike is situated within serpentinized peridotite (Fig. 2).

Table 2
Representative electron microprobe analyses of high-pressure and retrograde phases in metaquartzites

Sample	Phe	Phe	Phe	Grt	Grt	Grt	Grt	Gln	Gln	Chl	Chl	Bt
	EE3	J4	J4	EE3	EE3	J4	J4	EE3	EE3	J4	J4	J4
			Symplectite	Core	Rim	Core	Rim	Core	Rim	Core symplectite	Rim symplectite	Symplectite
wt.%												
SiO_2	53.4	52.4	53.0	36.8	37.3	36.9	37.1	57.9	55.4	29.2	29.5	39.6
TiO_2	0.08	0.06	0.07	<0.01	<0.01	<0.01	0.02	0.01	0.08	<0.01	0.04	0.02
Al_2O_3	21.4	22.3	22.2	20.0	20.3	20.2	20.5	7.66	5.41	19.0	17.9	15.9
Cr_2O_3	<0.01	0.04	0.05	0.02	<0.01	<0.01	<0.01	<0.01	0.05	0.05	<0.01	<0.01
Fe_2O_3				1.65	1.54	1.10	0.69	7.34	11.3			
FeO	4.34	4.28	4.31	24.6	30.7	25.2	34.8	7.98	7.18	21.5	20.8	16.9
MnO	0.01	0.01	0.04	12.2	5.23	10.5	0.95	0.04	0.26	0.61	0.58	0.47
CaO	<0.01	<0.01	<0.01	3.36	3.40	4.45	3.47	0.24	1.38	0.12	0.06	0.03
Na_2O	0.07	0.08	0.13	0.03	<0.01	0.05	0.02	7.41	6.50	0.08	0.05	0.14
K_2O	11.4	11.4	11.1	0.01	<0.01			0.03	0.02	0.14	0.10	10.0
H_2O	4.44	4.41	4.44					2.18	2.12	11.7	11.8	3.95
Sum	99.8	99.3	99.8	100.1	100.9	99.7	99.8	101.0	100.0	100.1	100.0	100.0
Cations normalized to	12 oxy	12 oxy	12 oxy	12 oxy 8 cations	12 oxy 8 cations	12 oxy 8 cations	12 oxy 8 cations	23 oxy 13 cat.+ Na+K	23 oxy 13 cat.+ Na+K	18 oxy	18 oxy	11 oxy 8 cations
Si	3.614	3.563	3.580	2.995	2.993	3.001	3.001	7.971	7.834	2.977	3.002	3.008
Ti	0.004	0.003	0.004				0.001	0.001	0.009		0.003	0.001
Al	1.705	1.787	1.767	1.914	1.922	1.939	1.956	1.244	0.901	2.288	2.153	1.421
Cr		0.002	0.003	0.001			0.002		0.005	0.004		
Fe^3				0.101	0.094	0.068	0.042	0.760	1.205			
Fe^2	0.245	0.244	0.244	1.672	2.056	1.717	2.353	0.919	0.849	1.836	1.772	1.074
Mn	0.001	0.001	0.003	0.837	0.355	0.723	0.065	0.004	0.031	0.052	0.050	0.030
Mg	0.463	0.438	0.446	0.182	0.287	0.157	0.275	2.101	2.167	2.677	2.920	1.466
Ca				0.293	0.292	0.388	0.301	0.035	0.209	0.014	0.007	0.002
Na	0.010	0.010	0.018	0.004	0.001	0.008	0.004	1.978	1.781	0.016	0.010	0.022
K	0.984	0.993	0.956	0.002	0.001			0.005	0.003	0.020	0.013	0.971
H	2.000	2.000	2.000					2.000	2.000	8.000	8.000	2.000
# cations	7.027	7.041	7.018	8.000	7.999	8.000	8.000	15.018	14.994	9.895	9.93	7.995
Mg# (Fe^{2+})	0.654	0.643	0.646	0.098	0.123	0.084	0.105	0.696	0.719	0.594	0.622	0.577
Mg# (Fe_{tot})	0.654	0.643	0.646	0.093	0.118	0.081	0.103	0.556	0.513	0.594	0.622	0.577
Fe^{3+}/Fe_{tot}				0.057	0.044	0.038	0.018	0.453	0.587			
Al(IV)	0.386	0.437	.0420	0.005	0.007	0.000	0.000	0.029	0.166			0.992
Al(VI)	1.319	1.350	1.347	1.909	1.915	1.939	1.956	1.214	0.735			0.428

Fe^{3+} and water content were calculated stoichiometrically (without measurement of F, Cl and other anions for water content estimation). (Phe=phengite, Grt=garnet, Gln=glaucophane, Mg-rieb=Mg-riebeckite, Chl=chlorite and Bt=biotite; oxy=oxygens).

Calculations of pseudosections were performed using DOMINO software (De Capitani and Brown, 1987). Using the relatively Fe-rich bulk composition (Fig. 9A) and calculating chloritoid and garnet compositions at P=2.4 GPa and T=560 °C results in Mg# of 0.54 and 0.33 for chloritoid and garnet, respectively. Small discrepancies between calculated and measured Mg# of chloritoid and garnet might be attributed to non-ideality of the Mg–Fe chloritoid solid solution and the unknown amount of chloritoid and/or garnet Fe^{3+}.

For the Mg-rich domains, the absence of chlorite implies minimum pressures of ~2.0 GPa at temperatures between 550 and 620 °C for the assemblage kyanite, chloritoid and talc (Fig. 9A). In Fe-richer domains, chlorite is stable to higher pressures at low temperatures. Most notably, garnet is stable to lower temperature and kyanite appears only above ~600 °C. The observed garnet+chloritoid+talc assemblage is stable only above 2.0 GPa and enlarges its stability field to lower temperatures at higher pressures (Fig. 9B). In agreement with our observations (Fig. 5), the computed phase diagrams show different phase relationships and thus provide some ideas of how much the local equilibria affects the topology of phase diagram sections, and suggesting

Table 3
Representative electron microprobe analyses of high-pressure parageneses and retrograde phases in gneiss B_{11}

Sample	Grt	Grt	Phe	Phe	Zo	Ilm	Ttn	Ep	Chl
	B11	B11	B11	B11	B11	B11	B11	B11	B11
	Core	Rim							
wt.%									
SiO_2	39.2	37.4	52.7	51.7	39.4	0.55	31.0	38.5	25.5
TiO_2	0.01	<0.01	0.13	0.14	0.03	51.8	38.4	0.12	0.09
Al_2O_3	21.6	20.6	24.5	25.9	29.5	<0.01	1.15	26.2	19.2
Cr_2O_3	0.04	<0.01	<0.01	0.01	0.08	0.04	0.06	<0.01	0.02
Fe_2O_3	0.50	0.20			4.61	0.58	0.15	8.93	
FeO	28.0	36.2	3.09	3.32		42.3	0.25		31.1
MnO	0.58	1.45	<0.01	<0.01	0.15	3.78	0.04	0.13	0.48
MgO	8.92	1.68	4.16	3.73	0.01	0.08	0.01	<0.01	12.0
CaO	1.79	2.95	0.02	0.01	23.9	0.67	28.3	23.6	0.02
Na_2O	0.01	0.06	0.08	0.05	0.01	<0.01	<0.01	<0.01	0.02
K_2O	<0.01	<0.01	10.6	10.7	0.03	<0.01	0.01	<0.01	0.02
H_2O			4.48	4.49	1.94		0.23	1.91	11.1
Sum	100.7	100.5	99.7	100.0	99.7	99.8	99.5	99.3	99.6
Cations normalized to	12 oxygens 8 cations	12 oxygens 8 cations	12 oxygens	12 oxygens	12 oxygens 1 OH	3 oxygens 2 cations	5 oxygens 3 cations	12 oxygens 1 OH	18 oxygens
Si	3.007	3.019	3.523	3.453	3.037	0.014	1.009	3.026	2.761
Ti			0.007	0.007	0.002	0.980	0.941	0.007	0.007
Al	1.954	1.959	1.930	2.042		2.678		2.428	2.451
Cr	0.003			0.001	0.005	0.001	0.002		0.001
Fe^3	0.029	0.012			0.268	0.011	0.004	0.529	
Fe^2	1.799	2.445	0.173	0.186		0.892	0.007		2.806
Mn	0.038	0.099			0.009	0.081	0.001	0.008	0.044
Mg	1.021	0.202	0.415	0.372	0.001	0.003	0.000		1.930
Ca	0.147	0.255	0.001	0.001	1.980	0.018	0.991	1.987	0.002
Na	0.001	0.009	0.011	0.006	0.002		0.000		0.004
K			0.900	0.912	0.003		0.000		0.002
H			2.000	2.00	1.000		0.050	1.000	8.000
# cations	8.000	8.000	6.961	6.979	7.984	2.000	3.000	7.985	10.009
Mg# (Fe^{2+})	0.362	0.076	0.706	0.667					0.407
Mg# (Fe_{tot})	0.358	0.076	0.706	0.667					0.407
Fe^{3+}/Fe_{tot}	0.016	0.005			1.000			1.000	
Al(IV)	0.000	0.000	0.477	0.547	0.000			0.000	
Al(VI)	1.954	1.959	1.423	1.495	2.678			2.428	

Fe^{3+} and water content were calculated stoichiometrically (without measurement of F, Cl and other anions for water content estimation). (Grt = garnet, Phe = phengite, Zo = Zoisite, Ilm = ilmenite, Ttn = titanite, Ep = epidote and Chl = chlorite; oxy = oxygens).

that the presence or absence of kyanite + talc + Mg-chloritoid assemblages in metagabbros is not necessarily a temperature indicator (cf. Kienast and Pognante, 1988).

In Ca-rich domains (former plagioclase sites, in fresh, unaltered Mg gabbros), the paragenesis zoisite + chloritoid + clinopyroxene ± garnet has been observed. Experimental investigations in the NCFMASH system have shown that such assemblages have a limited pressure stability of ~2.3 to 2.5 GPa (at 550 and 620 °C, respectively), above the stability field of amphibole and chlorite, but below the lawsonite stability (Poli and Schmidt, 1995), which is generally consistent with the above calculated values.

5.2. Thermobarometry of the metasedimentary cover (metaquartzites EE_3, J_4 and chlorite–phengite gneiss B_{11})

Although garnet is not homogeneous and shows a bell-shaped (prograde) zoning–with a decrease of Mn rimward and a near constant composition in the last 25 μm in the metaquartzites (Fig. 6A), and an inverse (retrograde) zonation in the chlorite–phengite gneiss (Fig. 6B)–textural relationships clearly suggest simultaneous growth of phengite and garnet rims in the gneiss. Thus, temperatures were estimated using Fe–Mg exchange equilibria in coexisting garnet–phengite pairs. In the absence of Fe^{3+} determinations, all Fe

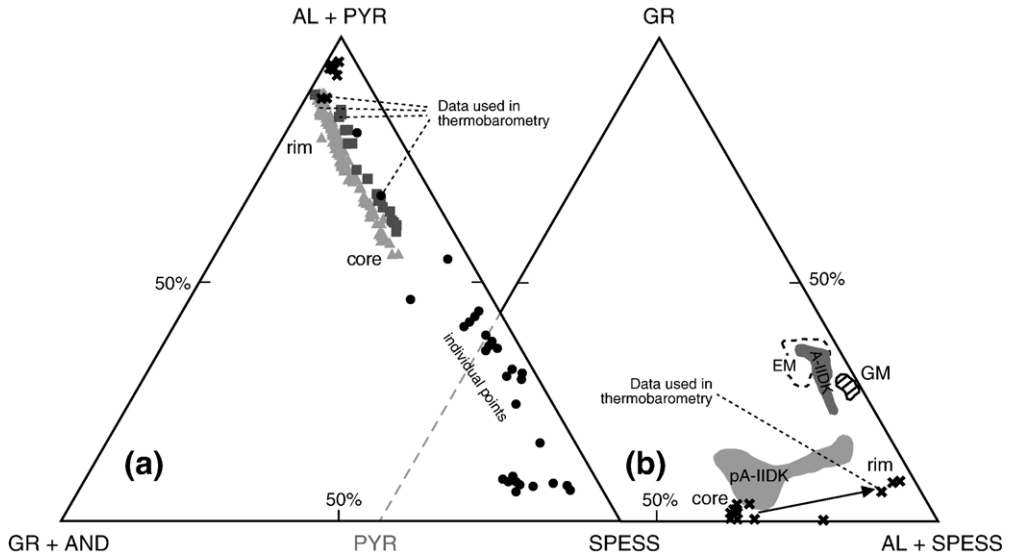

Fig. 8. (a) Compositional variation of garnets from metaquartzite EE_3 (squares), J_4 (triangles), chlorite–phengite gneiss B_{11} (crosses) and garnet data from Lagabrielle et al. (1989) (circles). Lagabrielle et al.'s (1989) samples were collected in the western part of the Lanzo cover, samples from the present study are from the northern area (for sample location, see Figs. 1 and 2). (b) Comparison between garnets from gneiss B_{11} (crosses), from pre-Alpine (pA) and Alpine (A) garnets of the seconda zona diorito-kinzigitica (IIDK), from gneiss minuti complex (GM) and from eclogitic micaschists (EM) from Pognante (1989).

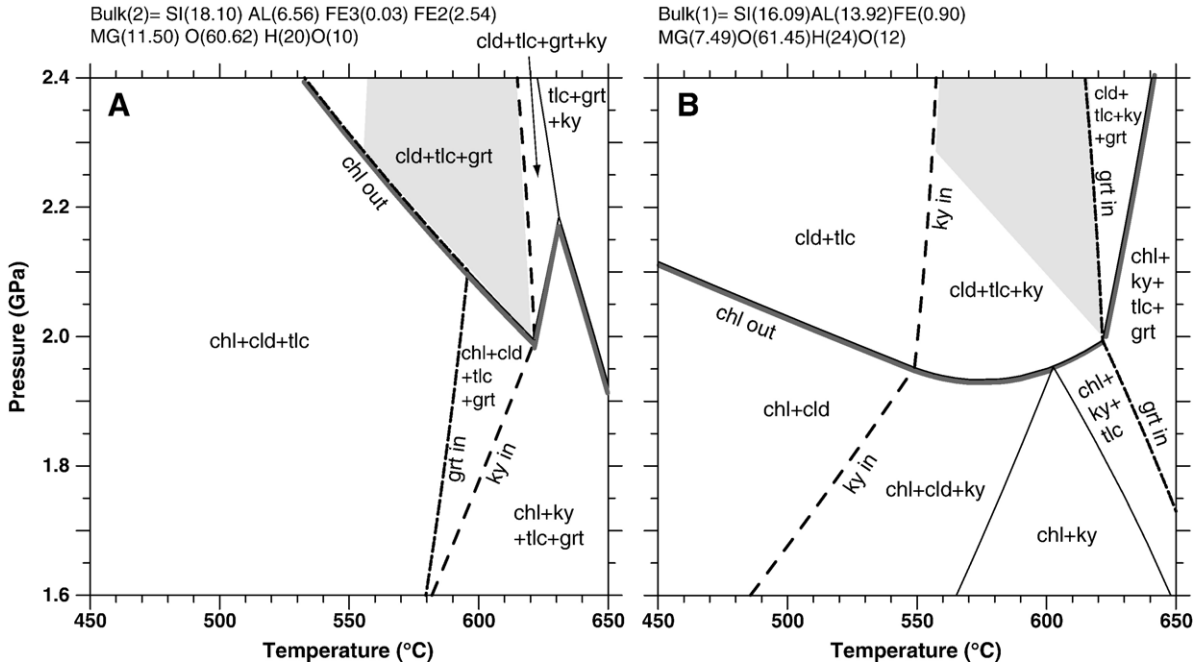

Fig. 9. Pressure–temperature diagrams illustrating topological relations between chloritoid (cld), chlorite (chl), talc (tlc), kyanite (ky) and garnet (grt) as a function of bulk compositions from two different Ca-poor domains in kyanite–talc metagabbro sample (O_2'). Reactions were calculated in the simplified FMASH system. (A) Reactions calculated for metagabbro domains dominated by garnet, chloritoid and talc. (B) Reactions calculated for metagabbro domains with kyanite, talc and chloritoid. Thick bold line indicates chlorite (chl)-out, dashed lines show first appearance of kyanite, stippled lines indicate first appearance of garnet. The shaded field indicates pressure–temperature conditions, which satisfy constraints from both subsystems. Note that in panel (A) garnet appears at lower T than kyanite, while the opposite has been found for panel (B). For further explanations, see text.

Table 4
Compilation of *P–T* estimates of the alpine metamorphic peak in the Lanzo massif, Lanzo cover, gneiss minuti complex (GM), eclogitic micaschist complex (EM) and seconda zona diorito-kinzigitica (IIDK) of the Sesia–Lanzo zone

Data from	Unit	Rock	HP metamorphic peak
Kienast and Pognante (1988)	Lanzo massif	Fe–Ti metagabbro	400–500 °C/1.5–1.8 GPa
Present study	Lanzo massif	Kyanite–talc metagabbro O_2'	550–620 °C/≥2.0 GPa
Present study	Lanzo cover (?)	Mn-rich metaquartzites EE_3, J_4	425–550 °C/>1.2 GPa
Lagabrielle et al. (1989)	Lanzo cover	Mn-rich metaquartzite	500–550 °C/~1.5 GPa
Lagabrielle et al. (1989) recalculated	Lanzo cover	Mn-rich metaquartzite	400–440 °C/0.9–1.1 GPa
Lagabrielle et al. (1989)	Lanzo cover	Jadeite gneiss	400–600 °C/1.5–2.0 GPa
Present study	Lanzo cover (?)	Chlorite–phengite gneiss B_{11}	510–590 °C/1.1–1.3 GPa
Williams and Compagnoni (1983)	GM	Leucocratic gneiss	500–550 °C/<1.3–1.5 GPa
Pognante et al. (1987)	GM	Leucocratic gneiss	400–475 °C/≥1.2 GPa
Pognante (1989)	GM	Orthogneiss	400–450 °C/≥1.1–1.2 GPa
Williams and Compagnoni (1983)	EM	Grt–Omp–Gln schists	~550 °C/>1.5 GPa
Pognante et al. (1987)	EM	Metabasites	500–550 °C/>1.4 GPa
Pognante (1989)	IIDK	Polymetamorphic paraschists	300–400 °C/0.8–1.0 GPa

Lagabrielle et al.'s (1989) data were recalculated with the geothermometer of Wu et al. (2002) and the geobarometer of Massonne and Szpurka (1997).

were assumed to be ferrous and therefore the calculated temperatures represent maximum values. The ferric-iron free formulation of the Wu et al. (2002, 2003) thermometer applied to the metaquartzites yields 460±30 °C (J_4) and 520±30 °C (EE_3), which are about 50 °C lower than calculations with the Green and Hellman (1982) thermometer (Table 4). Both values are comparable to previous estimates in other parts of the metasedimentary cover (Lagabrielle et al., 1989). The calculated values for the chlorite–phengite gneiss are 510 to 550 °C (Wu et al., 2002) and 450 ±20 °C with the Green and Hellman (1982) calibration, respectively.

Pressure estimates are subject to considerable uncertainty in the studied rocks since the tschermak exchange $MgSiAl_{-2}$ in phengite is not buffered by kyanite, a prerequisite for phengite barometry (Massonne and Szpurka, 1997). The finding of jadeite+quartz in gneiss in other parts of the Lanzo metasedimentary cover (Lagabrielle et al., 1989) nevertheless indicates that the metasediments equilibrated at pressures above 1.2 GPa in a temperature range of 500 to 550 °C. As illustrated in Fig. 10, pressure estimates for the studied samples are 0.9 to 1.3 GPa, based on the Si-content of phengite.

5.3. Retrograde reactions

Symplectite between glaucophane rims and phengite reveals a retrograde assemblage with biotite+chlorite+quartz (Fig. 4E). This assemblage was probably formed during the retrograde reaction phengite+talc=biotite+chlorite+quartz with complete consumption of talc. The formation of retrograde metamorphic parageneses is also documented in metaophicarbonate, where tremolite+calcite+antigorite formed at the expense of dolomite+diopside (Pelletier, 2003). According to Fig. 11, this would have

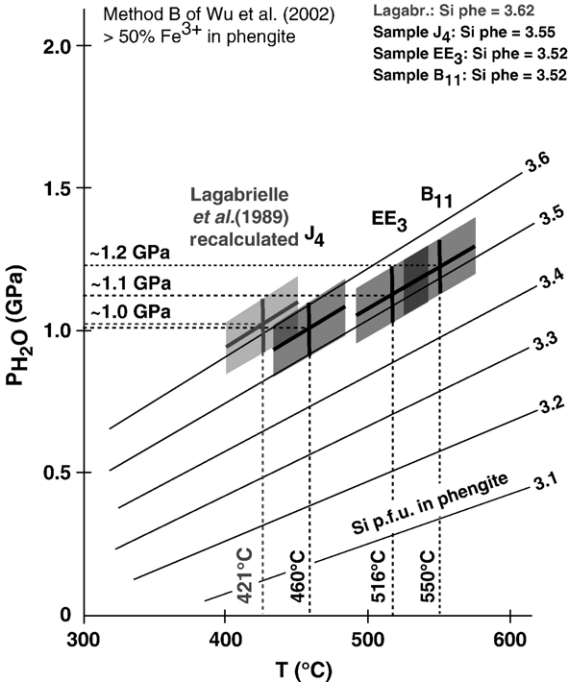

Fig. 10. High-pressure *P–T* conditions estimated for two metaquartzites (EE_3 and J_4) and for the gneiss (B_{11}) of the Lanzo metasedimentary cover. Phengite–garnet geothermometer (KFMASH system) of Wu et al. (2002) and Si content in muscovite geobarometer (KMASH system) of Massonne and Szpurka (1997) were used to define Si (a.p.f.u.) isopleths. Data of Lagabrielle et al. (1989) metaquartzite were also recalculated.

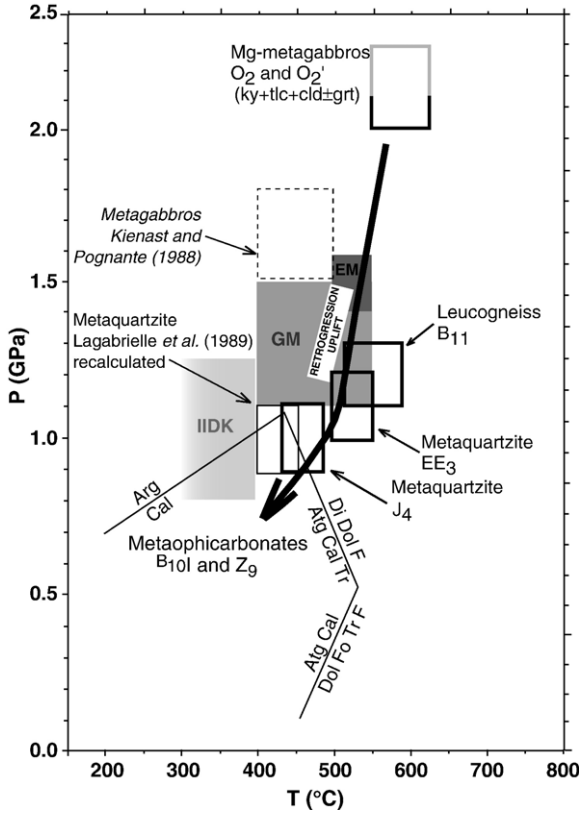

Fig. 11. Pressure–temperature diagram of available literature data for the Lanzo massif and the Sesia zone, compared to the results of this study. Broken line box: literature data from Kienast and Pognante (1988), continuous line boxes: present study. Bold line represents evaluated retrograde path. Light grey field corresponds to IIDK of Pognante (1989). Middle grey field corresponds to GM results and dark grey to EM (Williams and Compagnoni, 1983; Pognante et al., 1987; Pognante, 1989). Metaquartzites and gneiss results were obtained with Wu et al. (2002) garnet–phengite geothermometer and Massonne and Szpurka (1997) Si content in muscovite geobarometer. Stability field of metaophicarbonates is based on the Atg+Cal+Tr metamorphic assemblage of Connolly and Trommsdorff (1991). Pressure estimates of kyanite–talc–chloritoid are based on thermodynamic calculations (see Fig. 9). (Arg=aragonite, Cal=calcite, Di=diopside, Dol=dolomite, Atg=antigorite, Tr=tremolite, Fo=forsterite and F=fluid.)

happened at pressures below 1.0 GPa and at temperatures lower than 500 °C.

6. Discussion

6.1. Metamorphic equilibration of kyanite–talc metagabbro in the Lanzo peridotites

To the best of our knowledge, this is the first report on kyanite-bearing metagabbro from the Lanzo peridotite massif. Microtextural investigations have shown that kyanite only forms in some microchemical domains that are enriched in Al and Mg. In these microchemical domains, kyanite+talc are in equilibrium with chloritoid (Fig. 4A). In many of the metagabbroic rocks of the Lanzo peridotite massif, characteristic high-pressure chloritoid-bearing assemblages have been observed (e.g. Kienast and Pognante, 1988). Compositional and textural features discussed here indicate simultaneous growth of kyanite+talc+chloritoid and garnet+talc+chloritoid parageneses in different microchemical domains, corresponding to the shaded field in Fig. 9, above chlorite stability. Taking the paragenesis kyanite+talc+Mg-chloritoid (Mg# ~0.63) and comparing them to the FMASH experimental data of Koch-Müller and Wirth (2001), we obtain ~2.1 GPa at 540 °C and ~2.4 GPa at 600 °C. These estimates are in close agreement with our thermodynamic calculations (Fig. 9) and we therefore assume that the metamorphic peak in the Lanzo metagabbro was about 550 to 620 °C, with pressures in excess of 2.0 GPa (Fig. 11). These estimates are consistent with the presence of omphacite (jd55)+talc instead of glaucophane, suggesting pressures in excess of 1.7 GPa at 550 °C (Messiga et al., 1995).

However, glaucophane is a stable phase in some differentiated Fe–Ti metagabbros (Kienast and Pognante, 1988). Poli and Schmidt (1995) experimentally demonstrated that amphibole in mafic rocks disappears above 2.2 GPa, in the temperature range of 550 to 600 °C. Pawley and Holloway (1993) have proposed that amphibole and chloritoid may coexist over a narrow pressure interval between 2.2 and 2.5 GPa. Provided that local equilibrium is reached (as discussed by Kienast and Pognante, 1988), coexisting glaucophane and chloritoid in Fe–Ti metagabbros may provide an upper pressure limit for Lanzo gabbro dikes. To conclude, Lanzo kyanite–talc metagabbro has probably been subducted to pressures exceeding 2.0 GPa (but less than ~2.5 GPa), which corresponds to depths of 60 to 70 km.

6.2. Contrasting peak pressure records of basement and cover

The different garnet zoning pattern and the lack of a tschermak buffer for phengite induce large uncertainties in the pressure–temperature determinations of the metasediments. However, the mere fact that garnet rims seem to be equilibrated with phengite, independently of prograde or retrograde zoning pattern, indicates that garnet rims provide reliable temperature estimates. Our new *P–T* estimates for the Lanzo kyanite–talc metagabbro and its oceanic cover are

illustrated in Fig. 11, together with previous determinations from the Lanzo massif (Kienast and Pognante, 1988; Lagabrielle et al., 1989) and together with the various units of the Sesia zone (Pognante, 1989). The most striking feature is the observation of a marked pressure contrast between the basement rocks and its metasedimentary cover (Fig. 11). Several arguments might be put forward to explain this apparent discrepancy. One possibility is that the (schistose) metasedimentary rocks are affected by a much stronger retrograde blueschist and greenschist facies overprint than the (less deformed) basement rocks. This is supported by symplectite of biotite+chlorite +quartz (Fig. 4E) replacing phengite, and possibly talc. If so, talc+phengite might have been present at higher pressures. Together with glaucophane and zoisite relics, phengite+talc might have formed an eclogite facies paragenesis in the metasedimentary cover of the Lanzo peridotite, similar to the glaucophane+talc+phengite relics within metasediments from Lago di Cignana in the Zermatt-Saas Zone (Reinecke, 1998). An alternative scenario is metastability. Camacho et al. (2005) recently discussed the case that high-pressure metamorphism might has been rapid, but only in the presence of (hot) fluids the high-pressure metamorphism is registered by mineral assemblages. In this case, mantle rocks and metasedimentary cover were subducted to similar depth, but high-pressure transformations only occurred in the metagabbro dike, probably because fluids were provided by surrounding serpentinites. The metasedimentary cover thus received their (first) Alpine metamorphism during its return to the surface. Still another possibility is that both basement and metasedimentary cover record peak-pressures and thus the pressure difference may indicate that juxtaposition of the Lanzo peridotite and the oceanic cover is caused by post-subduction extensional faults. Ballèvre and Merle (1993) pointed out that 'pressure gaps' between several high-pressure units in the Western Alps could be explained by normal faults. Normal faults are probably required to explain the cold exhumation path from eclogite facies, blueschist facies to greenschist facies shown by several Western Alps high-pressure units (e.g. Pognante, 1989). Several cycles of compressional tectonics followed by extension are also preserved in the Austroalpine (e.g. Froitzheim et al., 1994). However, we were unable to find any evidence for substantial extensional tectonics in the study area, and therefore favor the hypotheses of metastability or variable retrogression between the basement and the metasedimentary cover.

6.3. Granulite facies relics on top of the Lanzo serpentinite?

Because garnet zoning profiles in the chlorite–phengite gneiss B_{11} from the Rio Ordagna illustrate a retrograde zoning and because the composition of the garnet cores shows a limited compositional variation (Fig. 6B), which is strikingly similar to garnets from the 'polymetamorphic paragneisses' of Pognante (1989), we tentatively propose that this paragneiss is a metamorphosed equivalent of granulite-facies rocks. Such granulite-facies rocks are widespread in the Sesia zone (IIDK: e.g. Pognante, 1989; Lardeaux and Spalla, 1991) and are interpreted as pre-Alpine granulite-facies lower crustal rocks. It is largely beyond the scope of this work to suggest a comprehensive mechanism for the occurrence of granulite facies relics within the serpentinized part of the Lanzo peridotite. Nevertheless, two possible scenarios are briefly addressed here. (i) Judging from regional-scale structural cross-sections presented by Spalla et al. (1983), it is possible that the granulite facies relics within the Lanzo peridotite are the result of polyphase thrusting and/or folding. This would imply that the northeastern contact between the Lanzo peridotite and the Sesia zone is entirely tectonic in origin, and the similarity of the oceanic cover of the continental Sesia unit and the Lanzo peridotite does not necessarily indicate that the two units were close to each other in pre-Alpine time. (ii) A second possibility is that the association of granulite facies relics on top of serpentinite, separated by an ophicarbonate zone is a primary feature that was established prior to the Alpine subduction cycle. This would imply that lower crustal continental and oceanic units were already juxtaposed in Mesozoic times, a typical feature of ocean–continent transition zones. Exhumed lower crustal and mantle rocks have been described in the Eastern Central Alps in Val Malenco (e.g. Müntener et al., 2000) and in the present-day Iberia margin (Manatschal et al., 2001). If this interpretation holds for the Sesia–Lanzo connection, it would have several important consequences for the origin and paleogeographic setting of the Lanzo peridotite, fostering the model of Bodinier et al. (1991) of a continental to oceanic mantle transition in the Lanzo peridotite.

7. Conclusions

The presence (or absence) of kyanite+talc in eclogite facies metagabbros in the Western Alps constitutes local equilibrium parageneses in different microchemical domains that are controlled by local bulk chemistry.

Thermodynamic calculations on different chemical subsystems indicate peak metamorphic conditions of 550 to 620 °C and 2.0 to 2.5 GPa for kyanite–talc metagabbro in the Lanzo peridotite. These conditions are substantially higher than those derived from the metasedimentary cover (500 to 550 °C and 0.9 to 1.3 GPa). The difference can best be explained by a complex retrograde metamorphic overprint erasing peak-metamorphic conditions or by metastability, leading to different peak metamorphic conditions. Such a 'metamorphic gradient' from the internal to the external part of the Lanzo peridotite is similar to the metamorphic structure of the Sesia zone indicating a common subduction history of the two units.

This study, together with the data from Lagabrielle et al. (1989) suggests that the Lanzo peridotite massif was at least partially covered by a thin sequence of Mesozoic sediments, and perhaps, by local remnants of granulite facies rocks. Any interpretation of the paleogeography of the continental Sesia zone and the oceanic Lanzo peridotite will have to be reevaluated, if a connection of lower continental crust and upper mantle peridotites can firmly be established. We tentatively propose that an ocean–continent transition origin for the Sesia–Lanzo connection best explains the geological and petrological constraints.

Acknowledgements

We thank A. Ulianov for analytical support and A. Berger, B. Lombardo, D. Castelli and two reviewers for comments, which helped to improve the manuscript. This work was financially supported by the Matthey-Dupraz foundation (LP) and by grants of the Swiss NSF (21-66923.01) to OM.

References

Ballèvre, M., Merle, O., 1993. The combin fault: compressional reactivation of a late Cretaceous–Early Tertiary detachment fault in the Western Alps. Schweizerische Mineralogische und Petrographische Mitteilungen 73, 205–223.

Beccaluva, L., Maciotta, G., Piccardo, G.B., Zeda, O., 1984. Petrology of lherzolitic rocks from the Northern Apennine ophiolites. Lithos 17, 299–316.

Berman, R., 1988. Internally-consistent thermodynamic data for minerals in the system Na_2O-K_2O-CaO-MgO-FeO-Fe_2O_3-Al_2O_3-SiO_2-TiO_2-H_2O-CO_2. American Mineralogist 29 (2), 445–522.

Berman, R., 1990. Mixing properties of Ca–Mg–Fe–Mn garnets. Journal of Petrology 75, 328–344.

Bodinier, J.L., 1988. Geochemistry and petrogenesis of the Lanzo peridotite body, western Alps. Tectonophysics 149, 67–88.

Bodinier, J.L., Guiraud, M., Dupuy, C., Dostal, J., 1986. Geochemistry of basic dikes in the Lanzo massif (Western Alps): petrogenetic and geodynamic implications. Tectonophysics 128, 77–95.

Bodinier, J.L., Menzies, M.A., Thirlwall, M.F., 1991. Continental to oceanic mantle transition: REE and Sr–Nd isotopic geochemistry of the Lanzo Lherzolite Massif. Journal of Petrology (Special Lherzolite Issue) 191–210.

Boudier, F., 1978. Structure and petrology of the Lanzo peridotite massif (Piedmont Alps). Geological Society of America Bulletin 89, 1574–1591.

Camacho, A., Lee, J.K.W., Hensen, B.J., Braun, J., 2005. Short-lived orogenic cycles and the eclogitization of cold crust by spasmodic hot fluids. Nature 435, 1191–1196.

Chopin, C., Schreyer, W., 1983. Magnesiocarpholite and magnesiochloritoid: two index minerals of pelitic blueschists and their preliminary phase relations in the model system MgO–Al_2O_3–SiO_2–H_2O. American Journal of Science 283-A, 72–96.

Compagnoni, R., 1977. The Sesia–Lanzo zone: high pressure–low temperature metamorphism in the Austroalpine continental margin. Rendiconti della Società Italiana di Mineralogia e Petrologia 33, 335–374.

Connolly, J.A.D., Trommsdorff, V., 1991. Petrogenetic grids for metacarbonate rocks: pressure–temperature phase-diagram projection for mixed-volatile systems. Contributions to Mineralogy and Petrology 108, 93–105.

Dal Piaz, G.V., 1999. The Austroalpine-Piedmont nappe stack and the puzzle of alpine Tethys. Memorie di Scienze Geologiche 51, 155–176.

De Capitani, C., Brown, T., 1987. The computation of chemical equilibrium in complex systems containing nonideal solutions. Geochimica et Cosmochimica Acta 51 (10), 2639–2652.

Défago, M., 2004. Relation pétrologique et structurale entre les ophiolites piémontaises et le massif de Lanzo (Piémont, Italie). Unpublished Diploma Thesis, University of Neuchâtel, Switzerland, 85 pp.

Desmons, J., Compagnoni, R., Cortesogno, L., Frey, M., Gaggero, L., Dallagiovanna, G., Seno, S., Radelli, L., 1999. Alpine metamorphism of the Western Alps: II. High-P/T and related pre-greenschist metamorphism. Schweizerische Mineralogische und Petrographische Mitteilungen 79, 111–134.

Evans, B.W., Trommsdorff, V., Richter, W., 1979. Petrology of an eclogite–metarodingite suite at Cima di Gagnone, Ticino, Switzerland. American Mineralogist 64, 15–31.

Froitzheim, N., Schmid, S.M., Conti, P., 1994. Repeated change from crustal shortening to orogen-parallel extension in the Austroalpine units of Graubünden. Eclogae Geologicae Helvetiae 87, 559–612.

Froitzheim, N., Schmid, S.M., Frey, M., 1996. Mesozoic paleogeography and the timing of eclogite facies metamorphism in the Alps: a working hypothesis. Eclogae Geologicae Helvetiae 89, 81–110.

Green, T.H., Hellman, L., 1982. Fe–Mg partitioning between coexisting garnet and phengite at high pressure, and comments on a garnet–phengite geothermometer. Lithos 15, 253–266.

Hunziker,. P., 2003. The stability of tri-octahedral Fe^{2+}–Mg–Al chlorite. A combined experimental and theoretical study. PhD thesis, University of Basel, Switzerland. 123 pp.

Inger, S., Ramsbotham, W., 1997. Syn-convergent exhumation implied by progressive deformation and metamorphism in the Valle dell'Orco transect, NW Italian Alps. Journal of the Geological Society (London) 154, 667–677.

Kienast, J.R., Pognante, U., 1988. Chloritoid-bearing assemblages in eclogitised metagabbros of the Lanzo peridotite body (western Italian Alps). Lithos 21, 1–11.

Koch-Müller, M., Wirth, R., 2001. An experimental study of the effect of iron on magnesiochloritoid–talc–clinochlore–kyanite stability. Contributions to Mineralogy and Petrology 141, 546–559.

Lagabrielle, Y., Cannat, M., 1990. Alpine Jurassic ophiolites resemble the modern central Atlantic basement. Geology 18, 309–322.

Lagabrielle, Y., Fudral, S., Kienast, J.R., 1989. La couverture océanique des ultrabasites de Lanzo (Alpes occidentales): arguments lithostratigraphiques et pétrologiques. Geodinamica Acta (Paris) 3, 43–55.

Lagabrielle, Y., Polino, R., Auzende, J.M., Blanchet, R., Caby, R., Fudral, S., Lemoine, M., Mével, C., Ohnenstetter, M., Robert, D., Tricart, P., 1984. Les témoins d'une tectonique intra-océanique dans le domaine téthysien: analyse des rapports entre les ophiolites et leur couverture métasédimentaire dans la zone piémontaise des Alpes franco-italiennes. Ofioliti 9, 67–88.

Lardeaux, J.M., Spalla, M.I., 1991. From granulites to eclogites in the Sesia zone (Italian Western Alps). A record of opening and closure of the Piemont ocean. Journal of Metamorphic Geology 9, 35–59.

Leake, B.E., Woolley, A.R., Birch, W.D., Burke, E.A.J., Ferraris, G., Grice, J.D., Hawthorne, F.C., Kisch, H., Krivovichev, V.G., Schumacher, J.C., Stephenson, N.C.N., Whittaker, E.J.W., 2004. Nomenclature of amphiboles: additions and revisions to the International Mineralogical Association's amphibole nomenclature. European Journal of Mineralogy 16, 191–196.

Lombardo, B., Pognante, U., 1982. Tectonic implications in the evolution of the Western Alps ophiolite metagabbros. Ofioliti 7, 371–394.

Manatschal, G., Froitzheim, N., Turrin, B., Rubenach, M., 2001. The role of detachment faulting in the formation of an ocean–continent transition: insights from the Iberia abyssal plain. In: Wilson, R.C. L., Withmarsh, R.B., Taylor, B., Froitzheim, N. (Eds.), Non-Volcanic Rifting of Continental Margins: A Comparison of Evidence From Land and Sea. Special Publication-Geological Society of London, vol. 187, pp. 405–428.

Massonne, H.S., Schreyer, W., 1989. Stability field of the high-pressure assemblage talc+phengite and two new phengite barometers. European Journal of Mineralogy 1, 391–410.

Massonne, H.S., Szpurka, Z., 1997. Thermodynamic properties of white micas on the basis of high-pressure experiments in the systems K_2O-MgO-Al_2O_3-SiO_2-H_2O and K_2O-FeO-Al_2O_3-SiO_2-H_2O. Lithos 41, 229–250.

Messiga, B., Scambelluri, M., Piccardo, G.B., 1995. Chloritoid-bearing assemblages in mafic systems and eclogite-facies hydration of Alpine Mg–Al metagabbros (Erro-Tobbio unit Ligurian Western Alps). European Journal of Mineralogy 7, 1149–1167.

Müntener, O., Piccardo, G.B., 2003. Melt migration in ophiolitic peridotites: the message from Alpine–Apennine peridotites and implications for embryonic ocean basins. In: Dilek, Y., Robinson, P.T. (Eds.), Ophiolites in Earth History. Special Publication-Geological Society of London, vol. 218, pp. 69–89.

Müntener, O., Hermann, J., Trommsdorff, V., 2000. Cooling history and exhumation of lower crustal granulites and upper mantle (Malenco Eastern Central Alps). Journal of Petrology 41, 175–200.

Nicolas, A., Etude pétrochimique des roches vertes et de leur minéraux entre Dora Maira et grand Paradis (Alpes, Piémontaises). PhD thesis, University of Grenoble, France. 299 pp.

Nicolas, A., 1974. Mise en place des péridotites de Lanzo (Alpes piémontaises); Relation avec tectonique et métamorphisme alpins; Conséquences géodynamiques. Schweizerische Mineralogische und Petrographische Mitteilungen 54, 449–460.

Nicolas, A., 1986. A melt extraction model based on structural studies in mantle peridotites. Journal of Petrology 27, 999–1022.

Parra, T., Vidal, O., Theye, T., 2005. Experimental data on the Tschermak substitution in Fe-chlorite. American Mineralogist 90, 359–370.

Pawley, A.R., Holloway, J.R., 1993. Water sources for subduction zone volcanism—new experimental constraints. Science 260 (5108), 664–667.

Pelletier, L., 2003. Relations entre une croûte océanique et sa couverture sédimentaire: L'exemple du massif de Lanzo (Alpes piémontaises, Italie). Unpublished Diploma Thesis. University of Neuchâtel, Switzerland. 83 pp.

Peters, T., Schwander, H., Trommsdorff, V., 1973. Assemblages among tephroite, pyroxmangite, rhodochrosite, quartz—experimental data and occurrences in Rhetic Alps. Contributions to Mineralogy and Petrology 42, 325–332.

Piccardo, G.B., Müntener, O., Zanetti, A., 2004. Alpine–Apennine ophiolitic peridotites: new concepts on their composition and evolution. Ofioliti 29 (1), 63–74.

Pognante, U., 1989. Lawsonite, blueschist and eclogite formation in the southern Sesia zone (western Alps Italy). European Journal of Mineralogy 1, 89–104.

Pognante, U., Lombardo, B., Venturelli, G., 1982. Petrology and geochemistry of Fe–Ti gabbros and plagiogranites from the Western Alps ophiolites. Schweizerische Mineralogische und Petrographische Mitteilungen 62, 457–472.

Pognante, U., Perotto, A., Rösli, U., Salino, C., Toscani, L., 1984. Petrologic evolution of some ophiolites from the Western Alps: the Lanzo and Civrari peridotites. Ofioliti 9, 54 (Suppl.).

Pognante, U., Rösli, U., Toscani, L., 1985. Petrology of ultramafic and mafic rocks from the Lanzo peridotite body (Western Alps). Lithos 18, 201–214.

Pognante, U., Talarico, F., Rastelli, N., Ferrati, N., 1987. High pressure metamorphism in the nappes of the Valle dell'Orco traverse (Western Alps collisional belt). Journal of Metamorphic Geology 5, 397–414.

Poli, S., Schmidt, M.W., 1995. H2O transport and release in subduction zones: experimental constraints on basaltic and andesitic systems. Journal of Geophysical Research 100 (22), 299–322, 314.

Reinecke, T., 1998. Prograde high- to ultrahigh-pressure metamorphism and exhumation of oceanic sediments at Lago di Cignana, Zermatt-Saas Zone, western Alps. Lithos 42, 147–189.

Rubatto, D., Gebauer, D., Compagnoni, R., 1999. Dating of eclogite-facies zircons: the age of Alpine metamorphism in the Sesia–Lanzo Zone (Western Alps). Earth and Planetary Science Letters 167, 141–158.

Spalla, M.I., De Maria, L., Gosso, G., Miletto, M., Pognante, U., 1983. Deformazione e metamorfismo della zona Sesia–Lanzo meridionale al contatto con la falda piemontese e con il massiccio di Lanzo, Alpi occidentali. Memorie della Societa Geologica Italiana 26, 499–514.

Vidal, O., Goffé, B., Bousquet, R., Parra, T., 1999. Calibration and testing of an empirical chloritoid-chlorite Mg–Fe exchange thermometer and thermodynamic data for daphnite. Journal of Metamorphic Geology 17, 25–39.

Vidal, O., Parra, T., Trotet, F., 2001. A thermodynamic model for Fe–Mg aluminous chlorite using data from phase equilibrium experiments and natural pelitic assemblages in the 100 degrees to 600 degrees C, 1 to 25 kb range. American Journal of Science 301, 557–592.

Vidal, O., Parra, T., Vieillard, P., 2005. Thermodynamic properties of the Tschermak solid solution in Fe-chlorite: application to natural

examples and possible role of oxidation. American Mineralogist 90, 347–358.

Wheeler, J., Butler, R.W.H., 1993. Evidence for extension in the western Alpine orogen: the contact between the oceanic Piemonte and overlying continental Sesia units. Earth and Planetary Science Letters 117, 457–474.

Williams, P., Compagnoni, R., 1983. Deformation and metamorphism in the Bard area of the Sesia–Lanzo Zone, Western Alps, during subduction and uplift. Journal of Metamorphic Geology 1, 117–140.

Wu, C.M., Wang, X.S., Yang, C.H., Geng, Y.S., Liu, F.L., 2002. Empirical muscovite geothermometry in metapelites. Lithos 62, 1–13.

Wu, C.M., Wang, X.S., Yang, C.H., Geng, Y.S., Liu, F.L., 2003. Erratum to "Empirical garnet-muscovite geothermometry in metapelites". Lithos 66, 291.